



Water dynamics in carbon nitride – a joint QENS, DFT and AIMD study.

20/01/2021

Speaker: Karolina Lisowska

Contributors: F. Foglia, A. J. Clancy, J. Berry-Gair, M. C. Wilding, T. Suter, T. S. Miller, K. Smith, F. Demmel, M. Appel, V. García Sakai, A. Sella, C. A. Howard, M. Tyagi, F. Corà, P. F. McMillan

Promising carbon based materials for synthetic membrane applications

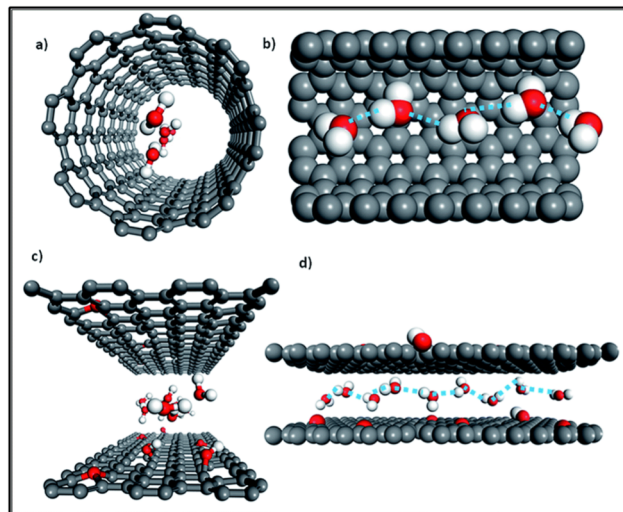


Fig. 1. Water transport in carbon nanotube CNT (a), (b) and through the nano-channels of graphene oxide GO (c), (d)

Chemical science, 8(3), pp.1701-1704. DOI: 10.1039/C6SC03909J

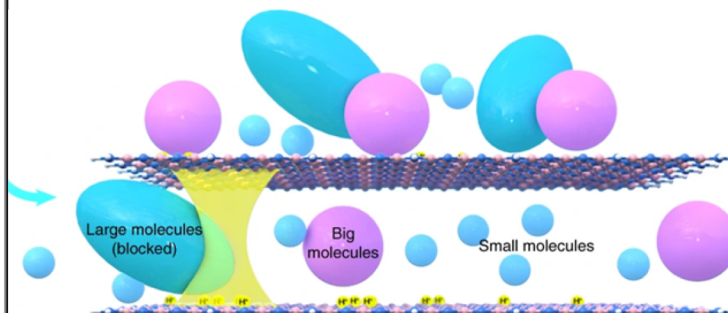


Fig. 2. Molecule transport through graphitic carbon nitride GCN. Intercalated anions used to control the interlayer spacing.

Nat Commun 10, 2500 (2019). <https://doi.org/10.1038/s41467-019-10381-z>

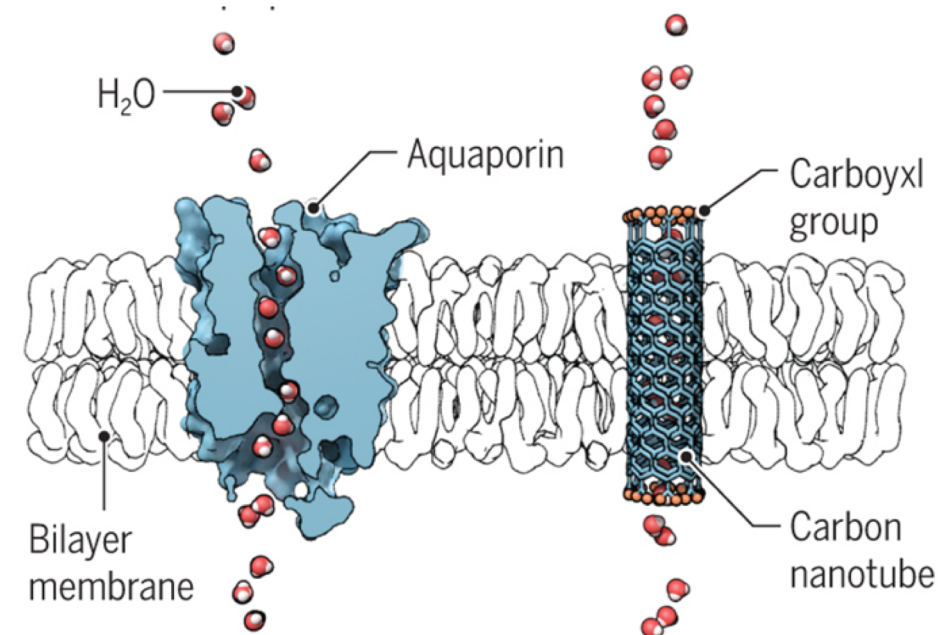


Fig. 3. Rapid water transport within lipid embedded CNTs analogous to directional water transport through AQP channels in cellular biomembranes

Science 25 Aug 2017: Vol. 357, Issue 6353, pp. 753 DOI: 10.1126/science.aao2440

- Water transport along the graphitic planes

- Water transport through the embedded channels

Nanoporous structure of the crystalline layered carbon nitride

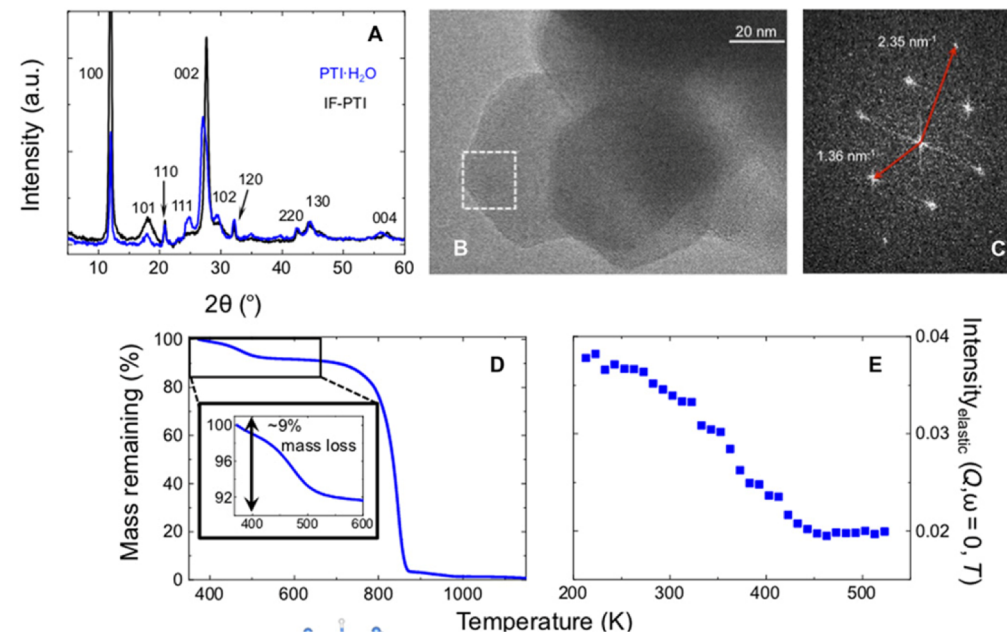
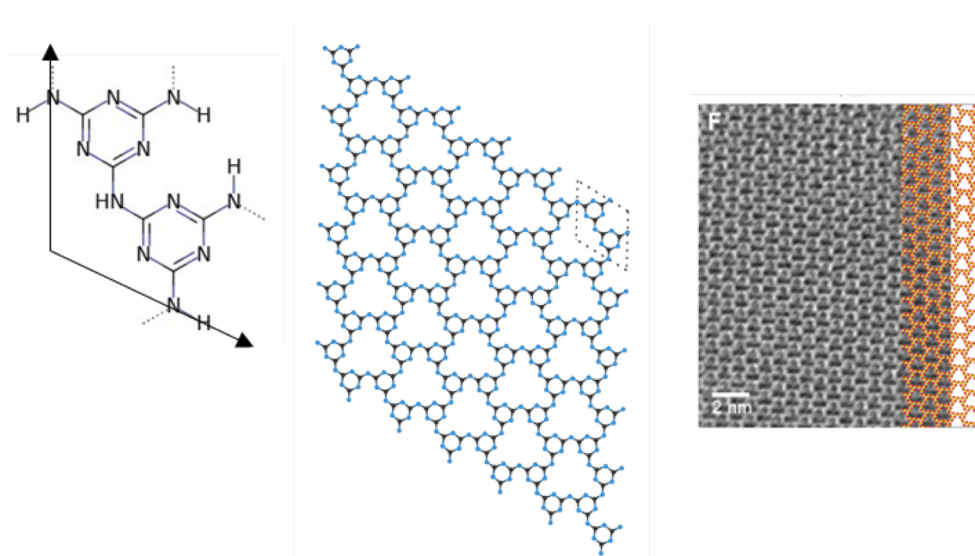


Fig. 4. Connectivity within a single PTI nanosheet. RIGHT: HRTEM image of single PTI sheet. DOI: 10.1126/sciadv.aay9851

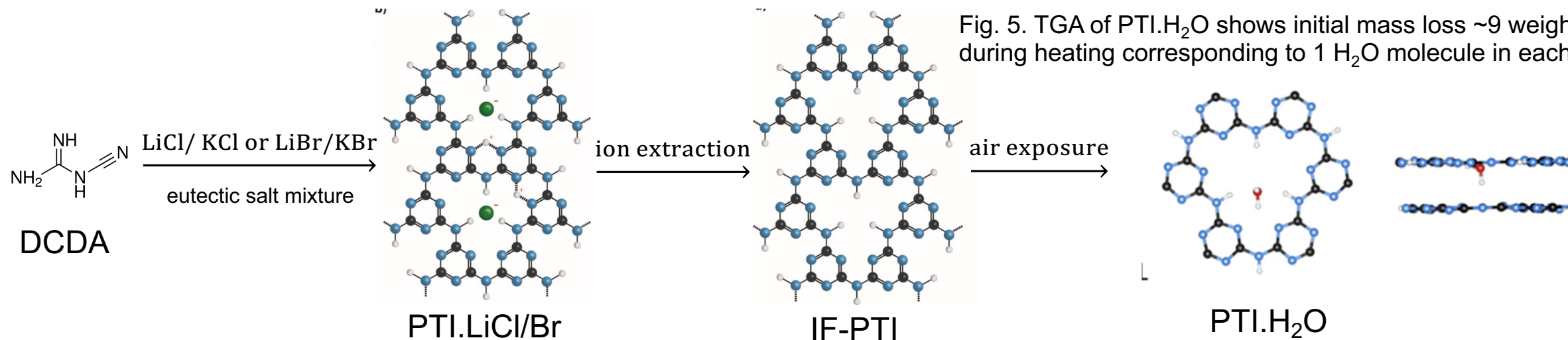
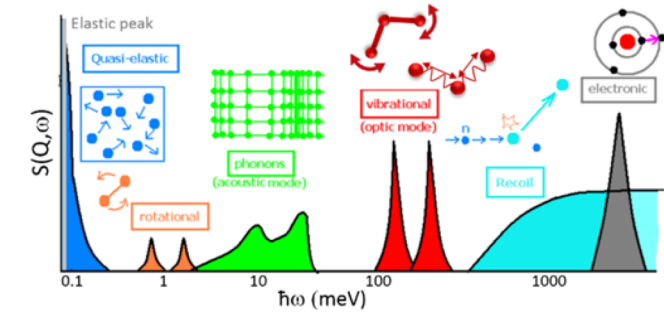


Fig. 5. TGA of PTI.H₂O shows initial mass loss ~9 weight % during heating corresponding to 1 H₂O molecule in each void.

Quasi Electron Neutron Scattering analysis of H₂O dynamics



- No Lorentzian broadening in dried (IF-PTI) sample
- N-H fs vibrational excitations below observed time scale
- Broadening in hydrated PTI (PTI.H₂O) at all probed time scales (ps-ns range)
- QENS profiles fitted with two Lorentzians
- Two types of water motion in PTI.H₂O

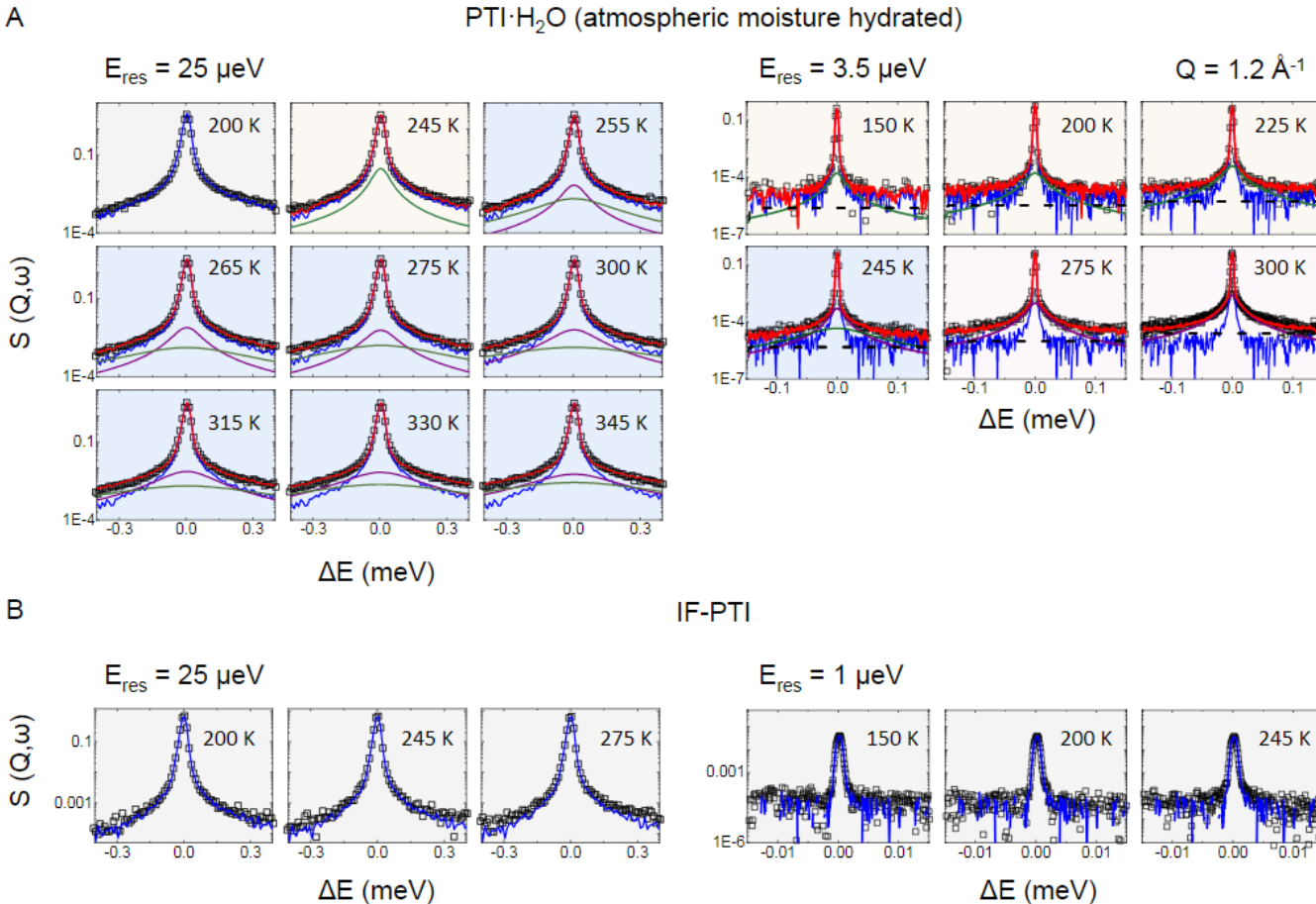


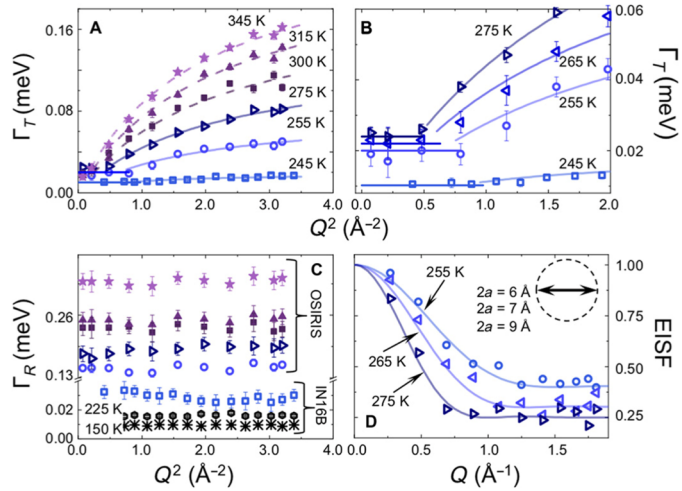
Fig. 6. QENS data for PTI before (IF-PTI) and after exposure to air (PTI.H₂O). Lorentzian broadening observed only for hydrated material.

Global fit, Data points, Localised relaxations, C-o-m translational diffusion, Background

Quasi Electron Neutron Scattering analysis of H₂O dynamics

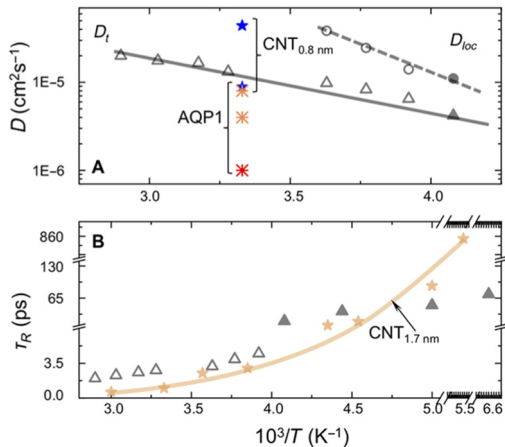
Narrow Lorentzian Component

Broader Lorentzian Component



- c -o-m diffusional displacement > 255 K
- Q-independent region at low Q dependant on T
- Nanoconfined H₂O dynamics at Q-independent region
- Q-independent Γ region at all Q
- Nanoconfined H₂O dynamics (spatially separated molecules constrained by H-bonding with local environment)
- Nanoconfined radius ~ 0.5 nm

Fig. 7. Analysis of half-width at half-maximum (HWHM, Γ) vs momentum transfer, Q



Membrane performance

- Translational D_t H₂O dynamics faster than transport within AQP channels
- Relaxation times from Q-independent broad component comparable with H₂O contained within CNTs

Fig. 8. Water dynamics in PTI.H₂O vs mobility in other nanoconfined environments (aquaporin AQP and carbon nanotubes CNT).

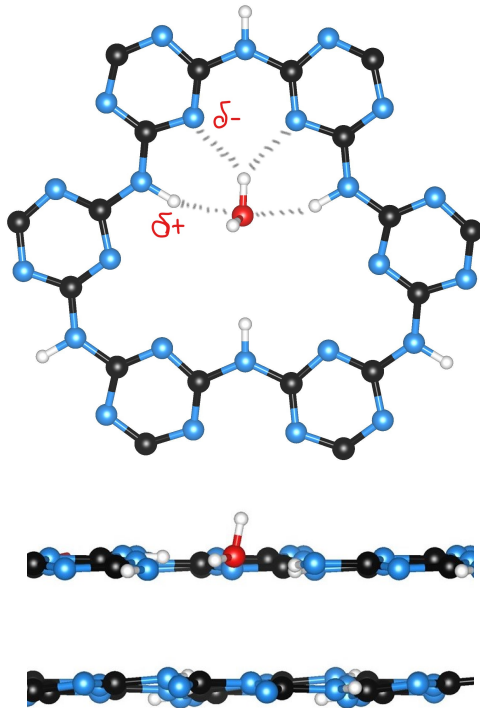
Density Functional Theory calculations

Experimental analysis
~9w% loss during heating
in TGA

→ Initial structure guess
1 H₂O molecule
per 1 nanopore

→ Geometry optimisation
DFT

→ Equilibrium geometry
Figure 9

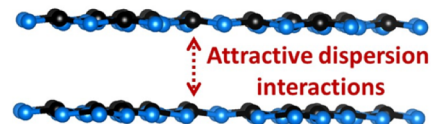


- Equilibrium H₂O position with O atom slightly above/below the PTI sheet
- One O-H bond nearly withing the PTI sheet, other perpendicular to the plane
- Geometry optimisation of dissociated H₂O returns neutral molecule
- Equilibrium H₂O position facilitated by OH···N and NH···O interactions with –N= and –NH- groups decorating the interior of the C₁₂N₁₂H₃ rings.

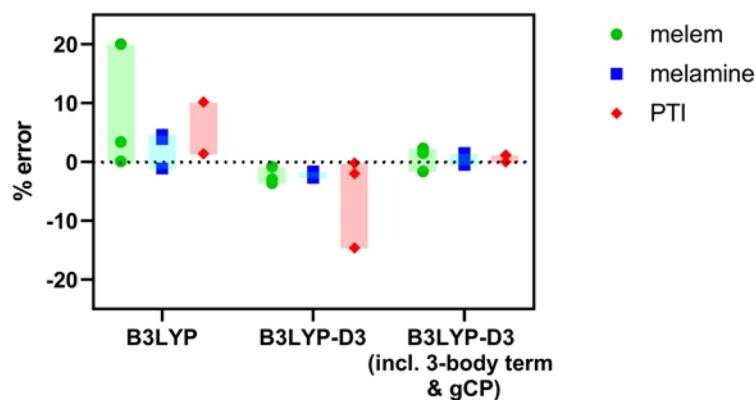
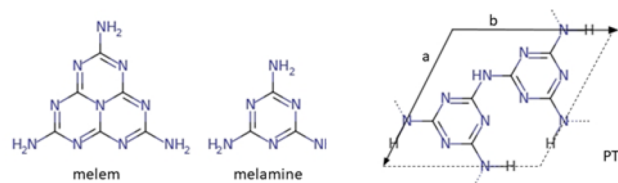
Fig. 9. Equilibrium location of H₂O molecule inside the intralayer pores.

Density Functional Theory calculations

Resolving the layer stacking in PTI



Precise description of the interlayer forces



- Structure with superimposed intralayer pores is maintained
- Channels available for water diffusion

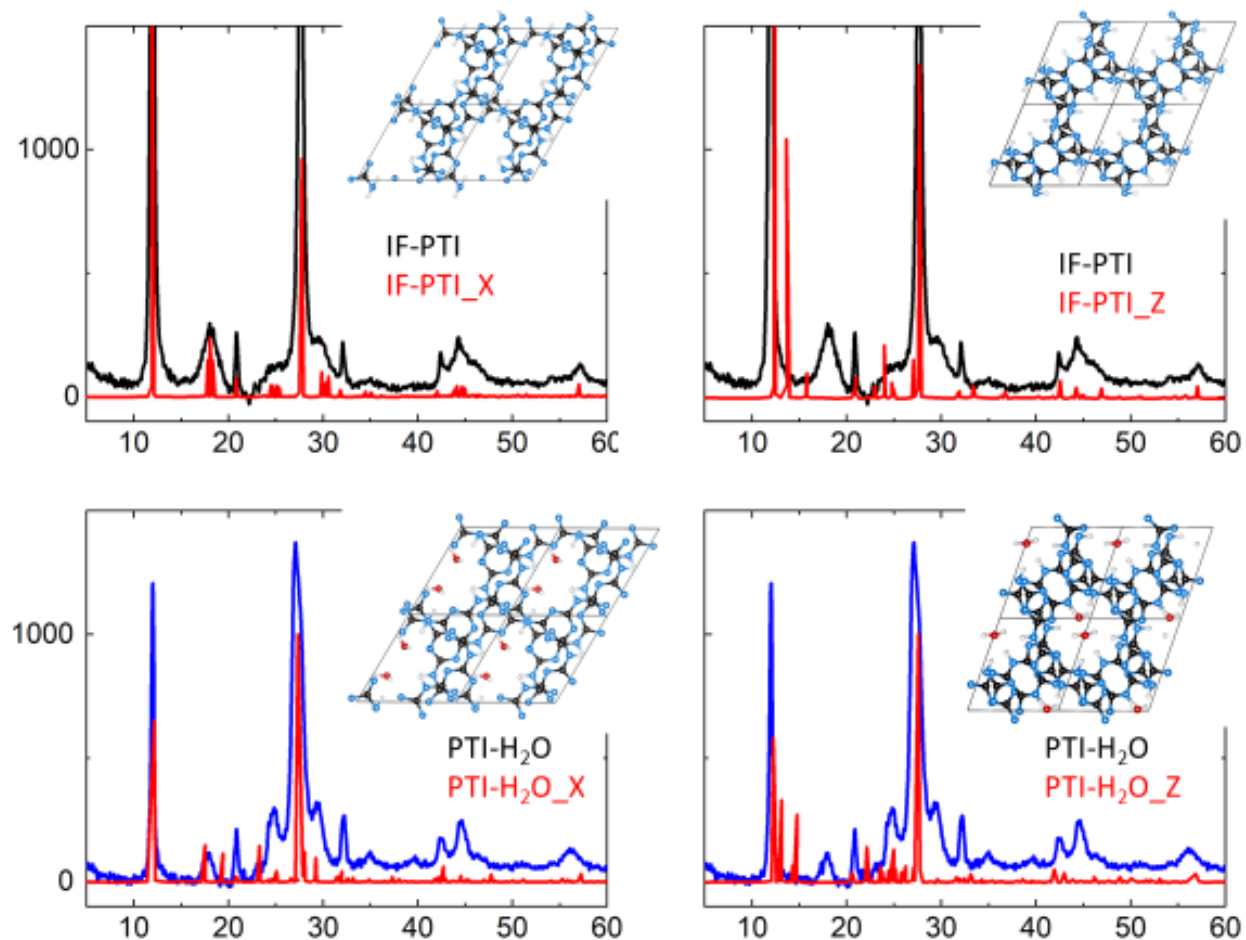


Fig.11. Error in the calc. lattice parameters vs level of dispersion description (no description/ disp. correction up to 2-body term/ disp. correction up to 3-body term + removal of artificial overbinding)

Fig.12. Experimental vs calculated XRD for IF-PTI and PTI.H₂O. Nearly isoenergetic structural variants ($\delta E = 1-7$ meV per C₂N₃H formula unit)

Ab Initio Molecular Modelling + series of constrained geometry optimisations (DFT)

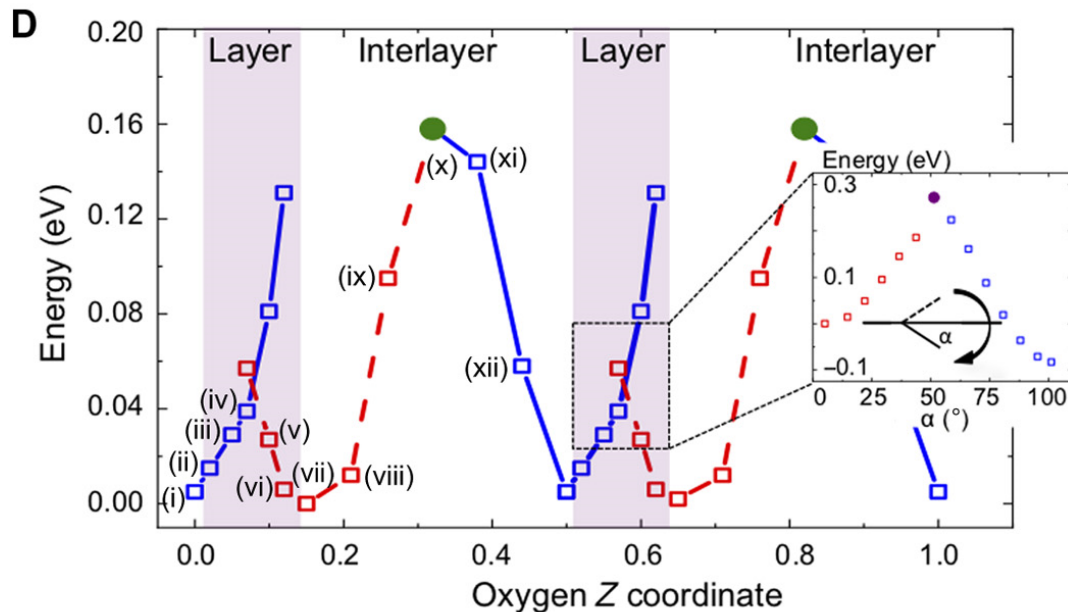
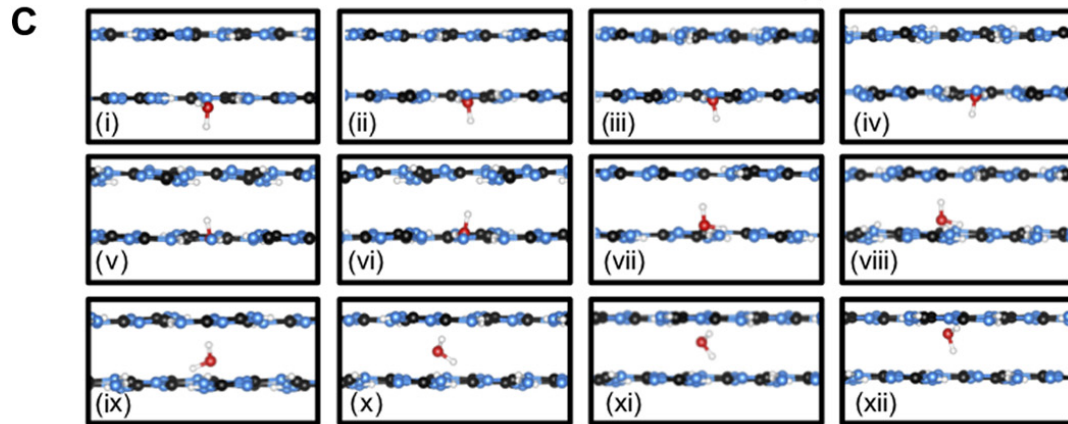


Fig. 13. Constrained geometry optimisations (DFT)

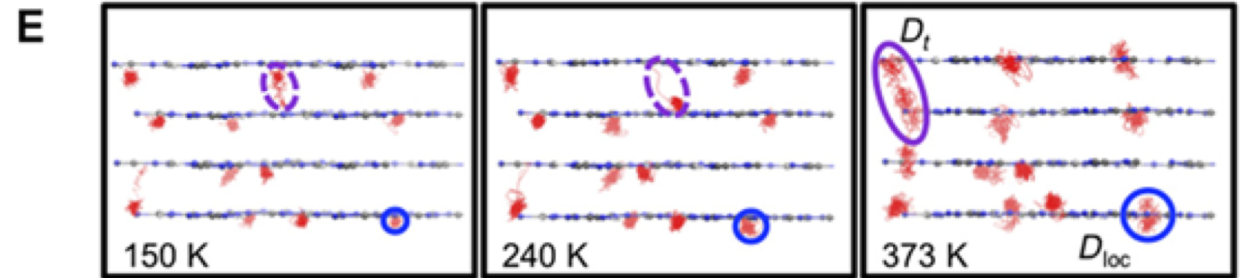


Fig. 13. AIMD simulations at different T values.

- Two energy barriers for translational diffusion (0.16, 0.3 eV)
- Sequential reversal in molecular orientation of H₂O
- AIMD confirms two types of water dynamics (D_{loc} at 150, 240K and D_t at 373 K)
- D_t over length scale up to 40 Å

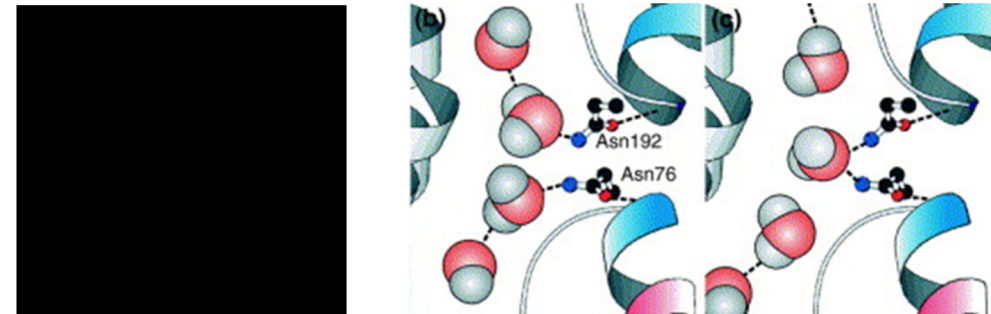


Fig. 14 Directed water transport in PTI vs in AQP channels

DOI: [HTTPS://DOI.ORG/10.1016/S0968-0004\(00\)01778-3](https://doi.org/10.1016/S0968-0004(00)01778-3)

QENS	DFT	AIMD
<ul style="list-style-type: none"> • Evidence for locally nanoconfined motions $\Gamma_R(Q^2)$ • Values for localized mobility D_{loc} • Evidence for c-o-m diffusion displacement of H₂O molecules $\Gamma_T(Q^2)$ • Estimate for translational diffusion coefficient D_t • Estimate of Debye-Waller radius and its relation to temperature • Temperature threshold for longer-range diffusional dynamics 	<ul style="list-style-type: none"> • Equilibrium geometry of IF-PTI and PTI.H₂O • Direction of H₂O diffusional displacement within PTI • Energetics of water transport • Evidence for H₂O reorientations during the transport 	<ul style="list-style-type: none"> • Evidence for locally nanoconfined motions • Evidence for c-o-m diffusion displacement of H₂O molecules • Estimate of Debye-Waller radius and its relation to temperature • Temperature threshold for longer-range diffusional dynamics

Thank you for listening!

[Foglia F. et al., “Aquaporin-like water transport in nanoporous crystalline layered carbon nitride”
Sci. Adv., 2020, 6, 39.](#)